

Overcoming Challenges of Direct Conversion Software Radio

OLEG PANFILOV, RON HICKLING, TONY TURGEON, WALTER BROOKS, KELLY
McCLELLAN, LLOYD LINDER

Terocelo, Inc.
6060 Sepulveda Blvd., Van Nuys, CA 91411
USA

<http://www.terocelo.com>

Abstract: - Direct conversion (from RF to complex I and Q baseband in one mixing step) architectures are increasingly popular as they enable substantially decrease implementation costs as well as reduce power consumption. However possible I and Q channels characteristics imbalance can cause significant performance degradations for systems using high order modulation such as 16-QAM and above typically used for high data rate transmission. Component aging, manufacturability and temperature variations can cause different channel latencies, signal amplitude variations or DC offsets. The paper describes proposed adaptive compensation of any possible sources of channel imbalances.

Key-Words: - adaptive imbalance compensation; direct conversion radio; quadrature channels

1. Introduction

The use of direct-conversion transceiver architectures substantially reduces component costs from one side and allows building frequency agile front ends capable to operate in multiband/multi-standard environments typical for nowadays communication from another. The unrelenting drive for higher efficiency of spectrum utilization in new communication services such as WiFi and WiMax brought sophisticated modulation techniques such as 64 QAM and OFDM (orthogonal frequency division multiplexing). However, there is the price to pay for higher efficiency. One of its components is a high degree of sensitivity of the associated receivers to channel imbalances between the In-phase (I) and Quadrature (Q) paths [1]. Phase mismatch occurs when phase difference between local oscillator signal for the In-phase and Quadrature channels is not exactly 90 degrees. Gain mismatch between I and Q channels may occur due to many factors such as different sensitivity channel components to temperature variations, different rate of component aging as well as different manufacturing tolerances of these components[2]-[8]. OFDM QAM systems suffer due to IQ imbalance in particular, because it uses both the main frequency and the image frequency to transmit different signals [1], [9]. So, the IQ imbalances can severely limit the achievable operating signal-to-noise ratio (SNR) at the receiver and, consequently, the supported constellation sizes and data rates. As the symbols are represented as complex numbers in constellation diagram, they can

be visualized as points on the complex plane. Upon reception of the signal, the demodulator examines the received symbol, which may have been corrupted by the channel or the receiver (e.g. additive white Gaussian noise, or interference). It selects, as its estimate of what was actually transmitted, the point on the constellation diagram that is closest (in a Euclidean distance sense) to that of the received symbol. Thus it will demodulate incorrectly if the corruption has caused the received symbol to move closer to another constellation point than the one transmitted. For the purpose of analyzing received signal quality, some types of corruption that are very evident in the constellation diagram are described below:

- Gaussian channel noise shows as fuzzy constellation points (see Fig 1a);
- Channel DC offset shifts a constellation point in this example right for the I channel offset and up for the Q channel (see Fig 1b);
- Phase imbalance rotates constellation points on the diagram relative to its ideal position as it is shown on Fig 1 c;
- Channel gain imbalance changes position of constellation points instead of being vertices of a square to the vertices of rectangular as it is shown in Fig 1d for two different cases.

The real and imaginary axes of a constellation diagram are often called the *in phase*, or I-axis and the *quadrature*, or Q-axis as it is shown in Fig. 1 for

the 4QAM. The *constellation points* on that diagram are a set of *modulation symbols* which comprise the *modulation alphabet*. For example, 16 QAM has an alphabet size equal to 16 and is represented by 4 bits ($2^4 = 16$). So, when an error symbol or bit rate has to be found, the relationship between symbol and its bit representation has to be taken into account.

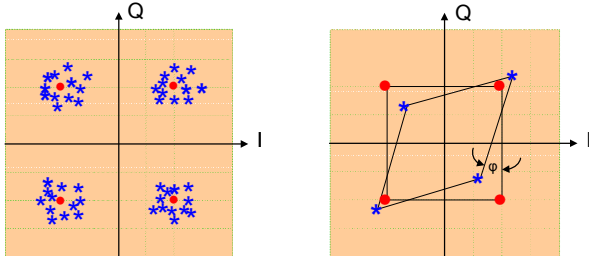


Fig. 1(a) Channel Noise

Fig. 1(b) Phase Imbalance

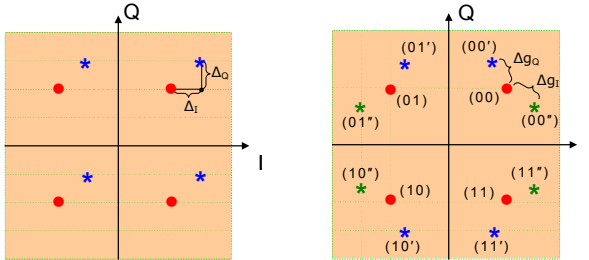


Fig. 1(c) DC Bias

Fig. 1 (d) Gain Imbalance of I and Q

The **error vector magnitude** or **EVM** is used in this paper as a measure to quantify the quality of a digital transmitter or receiver. A signal sent by an ideal transmitter and received by an ideal receiver would have all constellation points precisely at the ideal locations shown in Fig. 1 by red dots. As it was mentioned before various imperfections in the implementation cause the actual constellation points to deviate from the ideal locations. EVM is a measure of how far are the actual received data points from the ideal locations. Its length (magnitude) is defined as the Euclidean distance between the two points shown on Fig. 2.

The error vector magnitude is defined through a ratio of the mean square error vector $\sum_{m=1}^M |S_m - S_{0m}|^2$ to the mean square of the ideal symbol positions S_{0m} on a constellation diagram and can be expressed in dB or %

$$EVM [dB] = 10 \log \frac{\frac{1}{M} \sum_{m=1}^M |S_m - S_{0m}|^2}{\frac{1}{M} \sum_{m=1}^M |S_{0m}|^2} \quad (1)$$

$$EVM [%] = \sqrt{\frac{\frac{1}{M} \sum_{m=1}^M |S_m - S_{0m}|^2}{\frac{1}{M} \sum_{m=1}^M |S_{0m}|^2}} \cdot 100 \quad (2)$$

where M – number of unique symbols on the constellation diagram and the line over functions means a procedure of averaging.

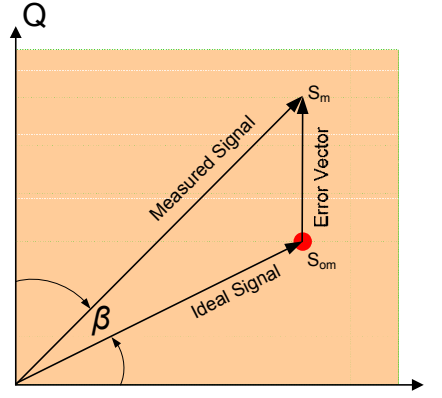


Fig. 2 The error vector

The major contribution of this paper is in developing simple methods of defining acceptable imbalances in phase and gain between I and Q channels as well as suggesting the ways how these imbalances can be adaptively compensated.

2. Sources of the Channel Imbalances

Phase mismatch occurs when phase difference between local oscillator signal for the In-phase and Quadrature (I and Q) channels is different from 90° as it is shown on Fig. 3. Without a loss of generality we will assume that a phase imbalance is due to an additional phase shift β in the in-phase (I) channel while both channel have different amplitude gains (A and B correspondingly). The end result of IQ imbalance in a quadrature receiver is the frequency interference aliasing into the desired signal band which reduces the dynamic range and degrades the receiver performance. It can be viewed as quazistationary over time [9], [10]. When the channel imbalance corrections are applied to the received signal, the phase and channel amplitude imbalances will require separate compensation as it will be shown later.

We will assume for our IQ imbalance analysis that the input signal $S(t)$ in Fig. 3 is the QAM signal having carrier frequency ω_0 . It can be represented as

$$S(t) = \text{Re}\{[I(t) + jQ(t)]e^{j\omega_0 t}\} \quad (3) \quad \text{or}$$

$$S(t) = I(t) \cos \omega_0 t - Q(t) \sin \omega_0 t \quad (4)$$

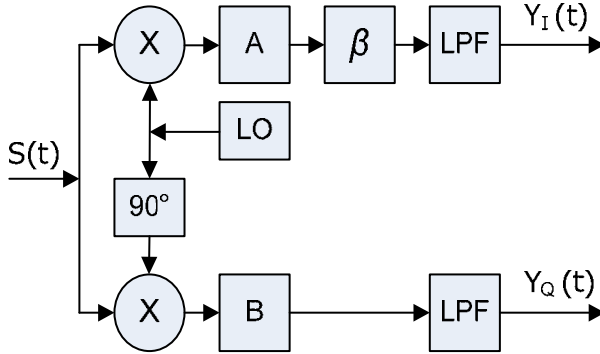


Fig. 3 Model of the I and Q channels gain and phase mismatch

After mixing with the signals from a local oscillator LO having ω_0 frequency the baseband signals for the in-phase $Y_I(t)$ and quadrature phase channels of a quadrature receiver with a low pass filter LPF will be

$$Y_I(t) = \frac{A}{2}[I(t) \cos \beta + Q(t) \sin \beta] \quad (5)$$

$$Y_Q(t) = \frac{B}{2}Q(t) \quad (6)$$

Equation (5) leads to one interesting observation. The phase imbalance β reduces the amplitude of signal in the in-phase channel and adds the $Q(t) \sin \beta$ component to the signal in the quadrature channel. Effectively it reduces the decision distance to the nearest neighbor point in the constellation diagram. The same effect is produced by the channel DC bias. The complex baseband signal may be obtained from Eqs (5),(6) as

$$W(t) = \frac{A}{2}I(t) \cos \beta + j \frac{Q(t)}{2}(A \sin \beta + B) \quad (7)$$

Presenting gain in the I channel as

$$A = B(1 + \frac{\epsilon}{1 - \epsilon}) \quad (8)$$

where the normalized gain imbalance in the I channel is

$$\epsilon = \frac{A - B}{A} \quad (9)$$

and the ideal undistorted baseband signal is

$$z(t) = \frac{B}{2}[I(t) + jQ(t)] \quad (10)$$

we can rewrite the received complex baseband signal in the form given in [13]

$$W(t) = \mu \cdot z(t) + \eta \cdot z^*(t) \quad (11)$$

Where distortion parameters relates to the physical channel imbalances as

$$\mu = \cos \beta + j\epsilon \sin \beta \quad (12)$$

$$\eta = \epsilon \cos \beta - j \sin \beta \quad (13)$$

and the $z^*(t)$ is the interference signal as a result of channel imbalances.

It is easy to show that the correlation coefficient ρ_{IQ} between $Y_I(t)$ and $Y_Q(t)$ signals is equal to $\sin \beta$

$$\rho_{IQ} = \sin \beta \quad (14)$$

So, by estimating the coefficient of correlation between signals in I and Q channels it is possible to find the phase bias between channels. The found phase shift β will be used in future for using its value for automatic phase imbalance compensation.

It is important to note that depending upon a transmitted symbol position on a constellation diagram the phase imbalance will have different impact on the symbol positions on that diagram. The value of $Q(t) \sin \beta$ in Eq (5) may be positive or negative. The random pattern of specific symbols arrival and the variable sign of $Q(t) \sin \beta$ component is the additional point in favor of the Gaussian distribution of signals in imbalanced channels. Such distribution is characterized by only its variance for the DC bias absence case. In the presence of thermal noise we can come up with the final equation describing the symbol error rate P_s as a function of effective signal-to-noise ratio (SNR) per symbol R obtained by modifying the one in [12]

$$P_s = 4(1 - \frac{1}{\sqrt{M}})Q\left(\sqrt{\frac{3R \cdot}{M - 1}}\right) \quad (15)$$

Here the probability integral Q can be written as

$$Q(x) = \frac{1}{2\pi} \int_x^\infty e^{-\frac{x^2}{2}} dx, \quad (16)$$

Effective signal-to-noise ratio is

$$R^{-1} = E^2 + \gamma^{-1} \quad (17)$$

E – EVM,

γ - symbol signal-to-channel thermal noise ratio.

It is clear from Eq (17) that depending on the level of channel imbalances or the thermal channel noise level one of them will dominate the symbol error rate. For small probability of bits in error it is easy to obtain the probability of bit error rate (BER) from (15) as a function of SNR per bit R_b

$$P_b = \frac{4}{\log_2 M} (1 - \frac{1}{\sqrt{M}})Q\left(\sqrt{\frac{3R_b \log_2 M \cdot}{M - 1}}\right) \quad (18)$$

A few words have to be said about the way how EVM can be defined. For the square QAM the EVM value E will be [10]

$$E^2 = \left| \frac{\eta}{\mu} \right|^2 \quad (19)$$

Substituting Eqs (12), (13) into Eq (19) we can obtain

$$E^2 \approx \varepsilon^2 \cos^2 2\beta + 0.25 \sin^2 2\beta \quad (20)$$

We have to note that the symbol errors will happen each time when erroneous symbol will be mistakenly interpreted as the transmitted ones regardless of the mistake origin, would it be thermal noise of different type of imbalances. So, the channel noise will just changes the shape of acceptable channel imbalances according to Eqs (17), (20)

$$\frac{\varepsilon^2 \cos^2 2\beta}{E^2 - \gamma^{-1}} + \frac{0.25 \sin^2 2\beta}{E^2 - \gamma^{-1}} = 1 \quad (21)$$

For small allowances for channel imbalances typical for high QAM modulation order Eq (21) can be reduced to the more familiar equation. of ellipse that practically becomes a circle of radius

$\sqrt{E^2 - \gamma^{-1}}$ for small β .

$$\frac{\varepsilon^2 \cos^2 2\beta}{E^2 - \gamma^{-1}} + \frac{\beta^2}{E^2 - \gamma^{-1}} = 1 \quad (22)$$

. Eq (22) shows that increase of phase imbalances stretches the main ellipse axes along the channel gain imbalance variable. Reduction of signal-to-channel noise ratio reduces both major and minor ellipse axes, i.e. reduces acceptable gain and phase imbalances. The set of plots shown on Figs. 4, 5 were generated based on Eqs (20), (18) for different

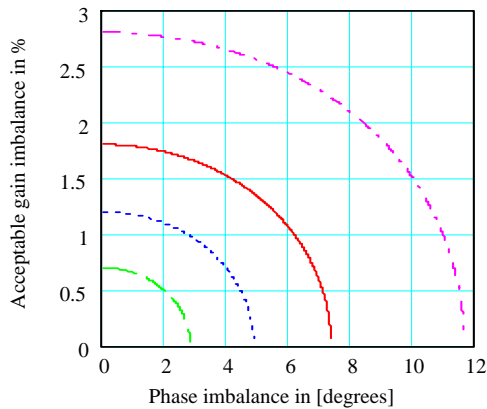


Fig. 4 Acceptable phase and channel gain imbalance

QAM systems operating in the environment with high signal-to-thermal noise ratio γ . The set of curves on Fig. 4 was done for the QAM systems providing the $BER=10^{-6}$. The acceptable set of values for channel imbalances belongs to the area under the plotted curves. For a example, 4QAM system will provide expected BER under the phase imbalance of 8° and the gain imbalance of 2% while

256 QAM providing 4 times higher throughput will require much stricter tolerances for the phase imbalance of less than 2° and gain imbalance less than 0.5%. Basically, Fig. 4 is a part of an ellipse of acceptable imbalances. Fig. 5 obtained from Eqs (18) shows the BER vs. EVM magnitude values expressed in % for QAM 4 (magenta), 16 (red), 64 (blue) and 256 (green) systems. As can be seen from Fig. 5 the BER values are most sensitive to the EVM values in the area of small BERs. It can be seen that to obtain $BER = 10^{-6}$ it is necessary to provide EVM values under 28,18,12 and 7% for 4,16,64 and 256 QAM correspondingly.

Since the DC offset as it would be shown later is relatively easy to compensate we will concentrate on the selection of acceptable range of phase and channel gain imbalances to meet the BER requirements in the environment where BER dominated by the channel imbalances. Say, we need a 64 QAM system providing $BER = 10^{-6}$. We can find from Fig. 5 that it will require EVM under 12%. Fig. 4 shows that a system providing gain imbalance under 1% and phase imbalance under 2.8° will meet our requirements.

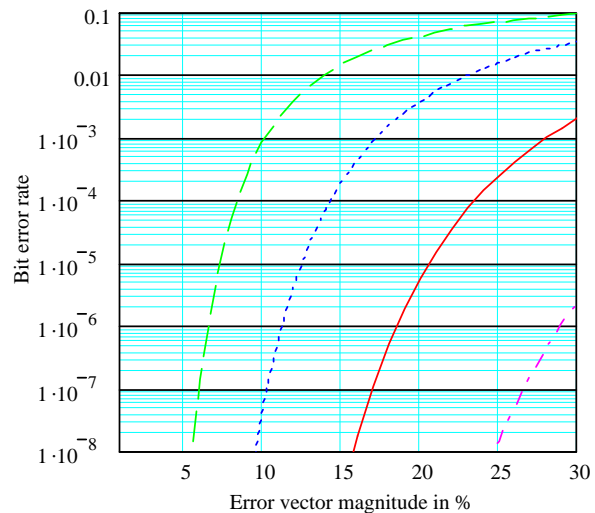


Fig. 5 BER vs EVM for the low thermal noise case

3. Cancelling I and Q channel Imbalances

The phase and amplitude imbalance compensation scheme shown on Fig.6 is based on the analysis of correlation properties of signals in I and Q channels. Here the I and Q channel signals are used to separately estimate phase and amplitude imbalance and correct it by multiplying channel signals on the weights proportional to estimated imbalances.

Correlation properties of I and Q channel signals are used by a correlation estimator to smooth out potential variations of input signals due to their fluctuations.

The required corrections for the amplitude and phase imbalance are adaptively estimated after receiving about 1000 samples.

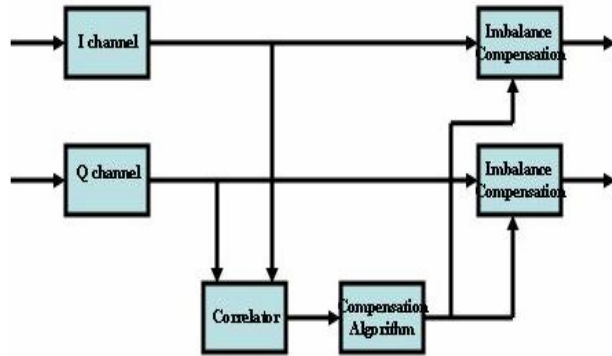


Fig. 6 Block diagram of the phase and amplitude imbalance compensation for I and Q channels

The impact of phase imbalance expressed in terms of bit error rates (BER) for 4QAM system is shown on Fig.7. Simulation showed that a system has about 5 dB penalties in BER values for the case of 30° degrees phase imbalance.

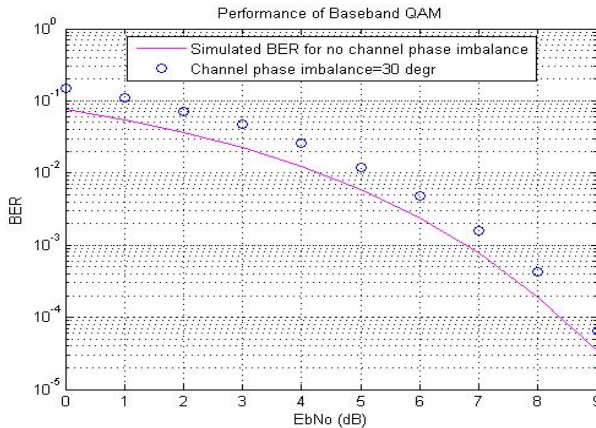


Fig. 7 Bit error rate vs. signal-to-noise ratio for the IQ channels

3. Experimental results

A photograph of the EVB101 evaluation board layout appears on Fig. 8. The Terocelo Lycon™ integrated circuit is located to the immediate right of the input transmission line (indicated by the red arrow in the Fig. 8). The layout of the EVB101 boards is such that multiple transmitters and receivers can be “daisy-chained” to create systems with multiple transmitters and/or multiple receivers (such as MIMO). A test configuration diagram of



Fig. 8 Layout of the EVB101-RX and EVB101-TX.

the EVB101-TX board appears in Fig.9.

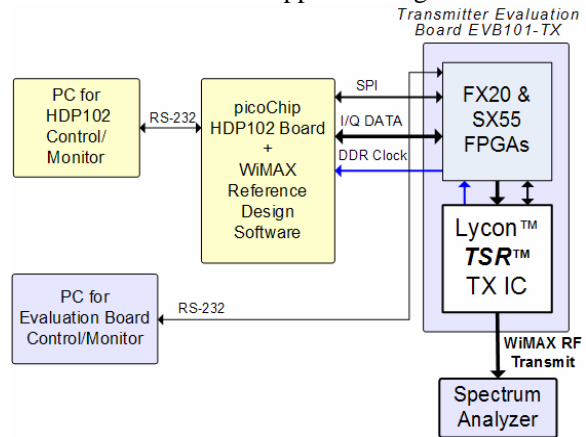


Fig. 9 Block diagram of the EVB101-TX board

In this configuration, the transmitter converts digital I/Q data (sampled baseband modulation waveform) to a WiMAX RF output signal. The transmitter evaluation board is controlled and monitored by a PC through a serial interface, including frequency of operation and filter characteristics. A picoChip baseband processor board generates the digital I/Q data, and is controlled and monitored by a PC through a separate serial interface. The WiMAX RF transmit signal from the EVB101-TX board is connected to an Agilent E4440A spectrum analyzer to measure the RF signal and baseband modulation. The measurements of major system parameters were done using the VSA Agilent software showing the major measurement results on the PC screen shown on Fig. 10. It can be seen from Fig. 10 that EVM=-39.9 dB or 1%, phase imbalance $\beta = 0.049^\circ$, gain imbalance = - 0.08 dB or 1%. Additional important information about SNR was derived from a spectrum analyzer. The picture of its screen is shown on Fig. 11. It is easy to find the SNR value keeping in mind that the 15 dB/division scale is shown there. Taken that into account we can see that

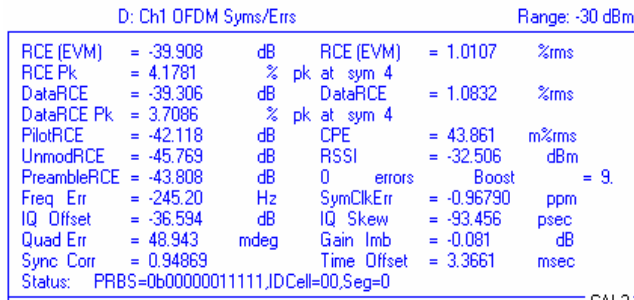


Fig. 10 The measured system data

$\gamma = 37$ dB. Since 64 QAM modulation was used representing one symbol with 8 bits, the bit energy per noise ratio $E_b N_0 = R_b = 28$ dB (37 dB – 10 log8). Substituting these values to Eq (17) it is clear that BER value in this specific case will be defined by channel thermal noises.

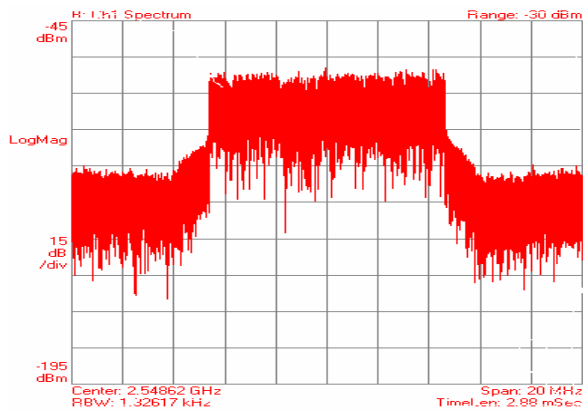


Fig. 11 Spectrum analyzer screen

5. Conclusions

One of the main challenges in building direct conversion software radio comes from necessity to maintain high orthogonality between the in-phase (I) and quadrature phase (Q) channels to prevent deterioration of signal-to-noise ratio leading to the increase in bit error rate. A simple method in estimating of acceptable level of IQ channels phase and gain imbalances was proposed based on the derivation of ellipse of acceptable channel imbalances linking it to the specified system bit error rate. The unpredictability of operational environment for direct conversion software radio makes the adaptive channel imbalance compensation a preferable choice. Using the divide and conquer approach it was proposed to adaptively compensate different imbalances – first DC offset by averaging the coming symbol stream in I and Q

channels, then averaging power of signals representing symbol coordinates in constellation diagram to compensate gain imbalances and then compensate phase imbalances extracting phase shift from correlation function of signals in I and Q channels.

References:

- [1] A. Tarighat, R. Bagheri, and A.H. Sayed “Compensation schemes and performance analysis of IQ inhabitants in OFDM receivers”, IEEE Transactions on Signal Processing, vol 53, Aug 2005
- [2] Proakis J. G. “Digital Communications”, 2001, McGraw-Hill
- [3] Jeffry Andrews “Interference Cancellation for Cellular Systems“, University of Texas, Austin, February 8, 2005
- [4] Maurer, L.; Chabrak, K.; Weigel, R.,” Design of mobile radio transceiver RFICs: current status and future trends”, First International Symposium on Control, Communications and Signal Processing, 2004 pp 53 – 56
- [5] Platz, J.; Strasser, G.; Feilkas, K.; Maurer, L.; Springer, A.,” A direct up-conversion transmitter with integrated prescaler for reconfigurable multi-band/multi-standard base stations”, Radio Frequency integrated Circuits (RFIC) Symposium, 2005. Digest of Papers. 2005 IEEE
- [6] Jurgen Helmschmidt, Eberhardt Schuler, et al “Reconfigurable Signal Processing in Wireless Terminals”, IEEE Proceedings of the conference Design Automation and Test in Europe, DATE-03.
- [7] Rainer Kokozinski, et al “The Evolution of Hardware Platforms for Mobile Software Definable Radio Terminals”, IEEE PIMRC2002.
- [8] Behzad Razavi “Design considerations for direct conversion receivers”, IEEE Trans. on circuits and systems, vol. 44, No 6, 1997
- [9] Chia-Liang Liu “Impact of I/Q imbalance on QPSK-OFDM-QAM detection”, IEEE Trans. On Consumer Electronics, Vol. 44, No3, 1998
- [10] Hassan Zarian, Vahid Vakili “Analytical BER Performance of M_QAM_OFDM Systems in the Presence of IQ Imbalances”, Proceedings of IFIP international conference on wireless and optical networks, July 2007, WOCN 2007, p 1-5